

Cosolvent Effects of Modified Supercritical Carbon Dioxide on Cross-Linked Poly(dimethylsiloxane)

M. F. Vincent,[†] S. G. Kazarian,[†] B. L. West,[†] J. A. Berkner,[†] F. V. Bright,[‡] C. L. Liotta,[†] and C. A. Eckert^{*,†}

Schools of Chemical Engineering and Chemistry and Biochemistry and Specialty Separations Center, Georgia Institute of Technology, Atlanta, Georgia 30332-0100, and Department of Chemistry, State University of New York at Buffalo, Buffalo, New York

Received: September 12, 1997; In Final Form: December 31, 1997

Supercritical fluid chromatography is a powerful technique for analysis, and it also provides a useful tool for the measurement of thermodynamic properties. For any application, the method involves equilibration between the mobile supercritical fluid phase and the polymeric stationary phase. The mobile-phase properties are often modified substantially with the addition of polar or protic cosolvents, but these adducts also cause changes in the stationary phases. In situ FTIR spectroscopy and the swelling of poly(dimethylsiloxane) (PDMS) are combined to quantify these changes due to partitioning of the cosolvent into and the swelling of the polymeric stationary phase as a function of fluid pressure. These results are used to evaluate the magnitude of the corrections for the changes in retention time of analytes, which affects both analytical methods and thermophysical property measurement.

Introduction

Supercritical fluid chromatography (SFC) is a powerful analytical technique often capable of separations inaccessible in either gas or liquid chromatography. Often the supercritical fluid mobile phase is modified by the addition of polar or protic cosolvents; but the effect of these on the stationary-phase properties, and concomitantly on the distribution coefficient of solutes between the phases, has not been well-investigated. Here we use spectroscopic techniques to study such effects and give quantitative measures of changes induced both in capacity factors in analysis and in thermophysical properties measured by chromatographic methods.

Supercritical fluids, especially carbon dioxide, are an attractive alternative for conventional liquid solvents. The physicochemical properties of a supercritical fluid are a strong function of pressure.^{1,2} Consequently, separations are easily accomplished by manipulating the system pressure.³ Also, chemical reactions^{4–11} may be tuned using the pressure-dependent properties of supercritical fluids. In addition, one of the most widely used supercritical fluids, carbon dioxide (scCO₂), is an environmentally “friendly” alternative to many conventional organic liquid solvents.

The “solvating” power and utility of neat scCO₂ can be expanded by the addition of cosolvents (entrainer or modifier).^{12–17} Cosolvents may be chosen to interact selectively with specific solutes through hydrogen bonding, dispersion forces, and ionic interactions. Thus, the addition of cosolvents yields another degree of freedom to utilize in tuning reactions¹⁸ and separations. For example, the solubility of hydroquinone in scCO₂ increases by 2 orders of magnitude when 2 mol % tri-*n*-butyl phosphate is added to the system.¹⁹

Despite the widespread use of SFC, it is difficult to tailor the mobile phase a priori for a particular separation. Currently,

a trial and error approach is used to identify an “optimal” set of experimental conditions (temperature, pressure, and cosolvent concentration) for a particular separation. Also, the effects of the cosolvent on stationary-phase properties are often ignored. To predict the conditions for an optimal separation and the effects of cosolvents on measured thermodynamic properties, the thermodynamics of the stationary phase in the presence of cosolvents is required. The pertinent cosolvent effects on the stationary phase are the following: (1) the presence of cosolvents will alter the swelling of the stationary phase as compared to pure scCO₂; (2) the absorption of cosolvents into a stationary phase may block active sites, thus precluding solute retention/interaction with the stationary phase; and (3) the cosolvent may act as part of the stationary phase, thus changing the chemical nature of the stationary phase. As an example, Parcher, et al.²⁰ used mass spectrometric tracer pulse chromatography to estimate the partitioning of cosolvent between the fluid phase and stationary phase. They reported that a C₁₈ bonded phase in contact with a 2 mol % methanol-modified CO₂ was composed of up to 25 mol % methanol in the near-critical region. The degree of partitioning decreases as the fluid density and temperature increase, but the concentration of methanol in the C₁₈ bonded phase always exceeded the concentration in the fluid phase. Clearly, an order of magnitude difference between stationary-phase and fluid-phase compositions is significant and can influence retention and thus capacity factors in SFC.

Supercritical fluid chromatography (SFC) also presents an attractive means to determine many thermodynamic properties (solute distribution coefficients, Henry’s law constants, Flory interaction parameters, partial molar volumes and enthalpies of the solute, and cosolvent effects) in scCO₂.^{20–27} It is more rapid than conventional methods and requires far less material.^{28–32} Using SFC, physicochemical properties may be obtained quickly (1 datum in 10 min) and with minimal solute (current SFC detectors are capable of nanogram sensitivity). Other benefits of using SFC include the ability to use impure solutes and

[†] Georgia Institute of Technology.

[‡] State University of New York at Buffalo.

measurement of multiple solutes simultaneously and does not require high-pressure sampling. However, corrections are required for stationary-phase effects when using SFC retention time techniques to determine thermodynamic properties.^{22,33–35}

The goal of this work is to characterize the behavior of a model stationary phase in the presence of cosolvent-modified supercritical carbon dioxide. Since the bulk of stationary phases in open tubular SFC are siloxane-based polymers, cross-linked poly(dimethylsiloxane) (PDMS) is the polymer chosen to represent the stationary phase. PDMS is chosen because it is the basis of most stationary phases. Functionalized siloxane-based polymers may exhibit very strong specific interactions with cosolvents, as well as with the carbon dioxide. We use FTIR spectroscopy to measure, in situ, the total concentration of cosolvent in the cross-linked PDMS film and in the fluid phase. This approach is analogous to the method we used to measure partitioning of other solutes between supercritical carbon dioxide and polymer phases.^{36–39} We also use the wealth of information available from FTIR spectra to elucidate the intermolecular interactions occurring in PDMS and in carbon dioxide and to determine the “polarity” of the stationary phase in the presence of cosolvent-modified carbon dioxide. To achieve this information, spectral features of the chosen cosolvents need to be separated from absorbances due to scCO₂ and cross-linked PDMS. The cosolvents utilized in the work are methanol (d₄), 2-propanol (d₈), and acetone (d₆). Together they represent the bulk of cosolvents utilized in the analytical chemistry literature.⁴⁰ Deuterated compounds are generally utilized^{21,36,41,42} since the combination bands of CO₂ ($\nu_3 + \nu_1$ and $\nu_3 + 2\nu_2$) obscure the $\nu(\text{O-H})$ stretching vibrations of methanol and 2-propanol, and the $\nu(\text{C-H})$ vibrations of PDMS obscure the $\nu(\text{C-H})$ vibrations of the undeuterated cosolvents. Fortunately, the bands corresponding to the $\nu(\text{O-D})$ and $\nu(\text{C-D})$ stretching mode vibrations of methanol (d₄) and 2-propanol (d₈) are separated from absorbances of PDMS and CO₂.

Theory

Capacity Factors. Roth⁴³ gives the relationships that express the effect of cosolvent concentration on the retention of a solute in supercritical fluid chromatography. Roth's work analyzes a two-phase, four-component system. The components are a solute (1), a stationary phase (2), a supercritical fluid (3), and a modifier (4). Equation 1 summarizes Roth's result, where the numerical subscripts refer to the component and subscripts “s” and “m” refer to the stationary and mobile phases, respectively.

$$\left(\frac{\partial \ln k_1}{\partial x_{4m}}\right) = \left(\frac{\partial \ln \varphi_{1m}^\infty}{\partial x_{4m}}\right)_{T,P,n_{2s}} - \zeta_{4m} - \frac{V_s}{V_m} \zeta'_{4s} \left(\frac{\partial x_{4s}}{\partial x_{4m}}\right)_{T,P,\sigma,n_{2s}} - \frac{1}{RT} \left(\frac{\partial \mu_{1s}^\infty}{\partial x_{4s}}\right)_{T,P,n_{2s}} \left(\frac{\partial x_{4s}}{\partial x_{4m}}\right)_{T,P,\sigma,n_{2s}} \quad (1)$$

where k_1 is the capacity factor of the solute, which is measured chromatographically and defined by eq 2,

$$k_1 = \frac{t_R - t_0}{t_0} \quad (2)$$

t_R and t_0 are the retention times of the solute and an unretained species, respectively; x_4 is the mole fraction of cosolvent; φ_{1m}^∞ is the infinite dilution fugacity coefficient of the solute in the mobile phase; V_s and V_m are the volumes of the stationary and mobile phases, respectively; ζ_{4m} is called the mixing

expansivity; ζ_{4m} and ζ_{4s} are defined below.

$$\zeta_{4m} = -\frac{1}{V_m} \left(\frac{\partial \bar{V}_m}{\partial x_{4m}}\right)_{T,P} \quad (3)$$

$$\zeta_{4s} = -\frac{1}{V_s} \left(\frac{\partial V_s}{\partial x_{4s}}\right)_{T,P,n_{2s}} \quad (4)$$

\bar{V}_m is the molar volume of the stationary phase and μ_{1s}^∞ is the infinite dilution chemical potential of the solute in the stationary phase. The use of eq 1 requires the mole fraction of cosolvent in the stationary phase. Since the stationary phase is typically a cross-linked elastomer, the mole fraction is not well-defined. A more meaningful variable is the volume fraction of solute in the stationary phase, ϕ_{4s} . Equation 5 results from Roth's analysis when volume fractions are utilized for the stationary-phase properties.

$$\left(\frac{\partial \ln k_1}{\partial x_{4m}}\right)_{T,P,n_{2s}} = \left(\frac{\partial \ln \varphi_{1m}^\infty}{\partial x_{4m}}\right)_{T,P,n_{2s}} - \zeta_{4m} - \frac{V_s}{V_m} \zeta'_{4s} \left(\frac{\partial \phi_{4s}}{\partial x_{4m}}\right)_{T,P,\sigma,n_{2s}} - \frac{1}{RT} \left(\frac{\partial \mu_{1s}^\infty}{\partial \phi_{4s}}\right)_{T,P,n_{2s}} \left(\frac{\partial \phi_{4s}}{\partial x_{4m}}\right)_{T,P,\sigma,n_{2s}} \quad (5)$$

ζ'_{4s} is termed the “cosolvent expansivity” and is defined in eq 6.

$$\zeta'_{4s} = -\phi_{3s} \left(\frac{\partial (1/\phi_{3s})}{\partial \phi_{4s}}\right)_{T,P,n_{2s}} \quad (6)$$

where ϕ_{3s} is the volume fraction of carbon dioxide in the stationary phase.

Equation 5 allows one to predict the cosolvent concentration dependence of the capacity factor. This prediction requires knowledge of the infinite dilution fugacity coefficient of the solute in the stationary phase and the mobile phase, the degree of swelling of the stationary phase induced by the cosolvent, and the extent of partitioning of the cosolvent between the stationary and mobile phases. The infinite dilution fugacity coefficients can be estimated from the appropriate equations of state. The stationary-phase swelling can be measured visually using polymer films similar to stationary-phase materials. The partitioning can be measured using the technique described in this paper. Therefore, one should be able to predict the cosolvent concentration dependence of a solute capacity factor using equations of state and equilibrium swelling and partitioning data.

Cosolvent Effect. The cosolvent effect is generally defined thermodynamically as the augmentation of solubility of a solute by the addition of a cosolvent to the supercritical fluid. If the solute is dilute, this can be expressed in terms of the solute's infinite dilution fugacity coefficient in the fluid phase ($\ln(\varphi_{1m}^\infty/\varphi_{1m,0}^\infty)$). The contributions of the individual terms to cosolvent effect are easier to see if we rearrange eq 5 and integrate over the cosolvent concentration, eq 7.

$$\ln \frac{\varphi_{1m}^\infty}{\varphi_{1m,0}^\infty} = \ln \frac{k_1}{k_{1,0}} + \int_0^{x_{4m}} \zeta_{4m} dx + \int_0^{x_{4m}} \frac{V_s}{V_m} \zeta'_{4s} \left(\frac{\partial \phi_{4s}}{\partial x_{4m}}\right) dx + \int_0^{x_{4m}} \frac{1}{RT} \left(\frac{\partial \mu_{1s}^\infty}{\partial \phi_{4s}}\right) \left(\frac{\partial \phi_{4s}}{\partial x_{4m}}\right) dx \quad (7)$$

where the subscript “0” refers to the condition of zero cosolvent

concentration. To obtain an accurate measurement of the cosolvent effect on the infinite dilution fugacity coefficients, there are four terms composed of six quantities that need to be determined. The ratio of capacity factors is measured using a chromatograph. The second term is an integral that involves, ζ_{4m} , which is a fluid-phase property that can be measured separately or calculated using an equation of state. The third term is an integral that is composed of three quantities, two of which are associated with the volumetric (swelling) behavior of the stationary phase, and the third term ($\partial\phi_{4s}/\partial x_{4m}$) is related to the partitioning of the cosolvent between PDMS and the fluid phase. The fourth term is composed of two quantities, one of which depends on the partitioning of the cosolvent between PDMS and the fluid phase ($\partial\phi_{4s}/\partial x_{4m}$), and the other depends on the chemical nature of the stationary phase in the presence of cosolvent ($\partial\mu_{1s}^\infty/\partial\phi_{4s}$). The third term shall be defined as the "swelling term", and the fourth term shall be defined as the "chemical term".

$$\text{swelling term} \equiv \int_0^{x_{4m}} \frac{V_s}{V_m} \zeta_{4s} \left(\frac{\partial\phi_{4s}}{\partial x_{4m}} \right) dx \quad (8)$$

$$\text{chemical term} \equiv \int_0^{x_{4m}} \frac{1}{RT} \left(\frac{\partial\mu_{1s}^\infty}{\partial\phi_{4s}} \right) \left(\frac{\partial\phi_{4s}}{\partial x_{4m}} \right) dx \quad (9)$$

In this work we evaluate the swelling and chemical terms, since the first term is measured chromatographically and the second term can be estimated using an equation of state. The cosolvent concentration dependence of three quantities is required to evaluate the two terms. The "cosolvent expansivity", ζ_{4s} , will be determined from the swelling behavior of the cross-linked PDMS in cosolvent-modified supercritical carbon dioxide. $\partial\phi_{4s}/\partial x_{4m}$ shall be determined by measuring the partition coefficient of the cosolvent. The partition coefficient, K_c , is defined in eq 10.

$$K_c \equiv \frac{C_{4s}}{C_{4m}} = \frac{\phi_{4s}}{V_4} \frac{\bar{V}_m}{x_{4m}} \quad (10)$$

where C_{4s} and C_{4m} are the concentrations of the cosolvent in the stationary and mobile phases, respectively. \bar{V}_4 is the molar volume of the cosolvent, and \bar{V}_m is the molar volume of the mobile phase. The cosolvent volume fraction dependence of the chemical potential of the solute ($\partial\mu_{1s}^\infty/\partial\phi_{4s}$) shall be determined from the Flory–Huggins equation of state.^{44,45}

Flory–Huggins Equation of State. The free energy of mixing, ΔG_M , is given by eq 11.

$$\Delta G_M = \Delta H_M - T\Delta S_M^* = kT \left(\sum_i \sum_{j>i} n_i \phi_j \chi_{ij} + \sum_i n_i \ln \phi_i \right) \quad (11)$$

where ΔH_M and ΔS_M^* are the enthalpy and configurational entropy of mixing, respectively, n_i is the number of i molecules, and χ_{ij} is the Flory–Huggins pair interaction parameter, which characterizes the interaction energy between i and j molecules divided by kT .⁴⁵ The chemical potential of species i , μ_i , relative to the reference state, μ_i^0 , is calculated by differentiating eq 11 with respect to n_i . The result is given in eq 12.

$$\mu_i - \mu_i^0 = RT \left[\ln \phi_i + (1 - \phi_i) \left(1 + \sum_{j \neq i} \chi_{ij} \phi_j \right) - \sum_{j \neq i} \frac{\phi_j}{x_{j,i} \chi_{j,i} k} \left(1 + \chi_{j,k} \phi_k \right) + \frac{\gamma_c \rho_P \bar{V}_i}{2} \left(\phi_1^{1/3} - \frac{\phi_1}{2} \right) \right] \quad (12)$$

where $x_{j,i}$ is the ratio of the molar volume of species j to molar volume of species i , γ_c is the degree of cross-linking (mol/g polymer), and ρ_P is the density of the unswollen PDMS. The last term in eq 12 is the contribution of the elastic free energy to the chemical potential.^{46,47} This expression allows the chemical potential of species i to be determined in a multicomponent mixture with binary interaction data.

Experimental Section

Apparatus. The optical bench was a Nicolet Impact 400D FTIR spectrometer using Omnic 2.0 operating software. The detector was a liquid-nitrogen-cooled MCT detector, and the resolution was 2 cm^{-1} . A special high-pressure cell was used for all spectroscopic measurements.^{36,37,39,42,48} This cell contained two parallel paths that allowed measurement of polymer-phase and fluid-phase spectra separately under identical conditions. Agitation was supplied via three independent magnetic stir bars inside the cell. A Jerguson level site gauge (model 11-T-32, Jerguson Gage & Valve Co.) with glass windows was used to observe the swelling of the PDMS films.

Material. Methyl-terminated PDMS (average molecular weight 302 000) was purchased from United Chemical Technologies, Inc., Petrarch Silanes & Silicones. The deuterated cosolvents, methanol- d_4 (99.8% isotope purity), 2-propanol- d_8 (99+% isotope purity), and acetone- d_6 (99.5% isotopic purity), were purchased from Aldrich Chemical Co. Undeuterated cosolvents, methanol (99.8%, ACS reagent), 2-propanol (99.5%, ACS reagent), and acetone (99.5%, ACS reagent), were also purchased from Aldrich Chemical Co. (Deuterated cosolvents were used in the spectroscopic measurements. The swelling experiments were performed with undeuterated cosolvents.) SFC grade carbon dioxide (99.99% purity) was purchased from Matheson. Trace H_2O was removed from the carbon dioxide using molecular sieves supplied by Matheson.

Polymer Film Preparation. The polymer films were prepared by cross-linking PDMS using benzoyl peroxide. A 27.075-g sample of PDMS and 2.988 g of benzoyl peroxide were dissolved in 125 mL of dichloromethane. Glass slides were then dipped in the mixture and allowed to dry in air. The polymer-covered slides were then cured at 130°C for 15 h. Unreacted benzoyl peroxide, benzoic acid, and un-cross-linked polymer were removed by successive washes in dichloromethane. Residual dichloromethane was removed by vacuum drying. The degree of cross-linking was determined to be $1 \times 10^{-4} \text{ mol/(g polymer)}$ from equilibrium swelling in benzene^{45,47,49–51} at 25°C .

High-Pressure Swelling Experiments. The method was similar to those described in the literature.^{52,53} A PDMS film was cut from a clean and dry polymer sheet, as prepared above. The film was cut in the shape of a half-barbell and secured in the polymer film holder; see Figure 1. The polymer film holder was designed so that it swung freely and always remained absolutely vertical, irrespective of the orientation of the Jerguson site gauge. The temperature was controlled to within $\pm 0.2^\circ\text{C}$ using electric heating tape (Omega Technologies Company) and a Precision Temperature Controller (model 123, Bayley Instrument Co.). Prior to any measurements the virgin polymer film was extracted with scCO_2 (41.5°C and 175 bar) for 15 h to remove any remaining impurities. The unswollen length, l_0 , was determined, after evacuating the cell, by measuring the distance between the interior points A and B (see Figure 1) using a cathetometer (Gaertner Scientific Corp., Chicago). By measuring the distance using the interior points A and B, we eliminate any distortion that may occur due to curling of the

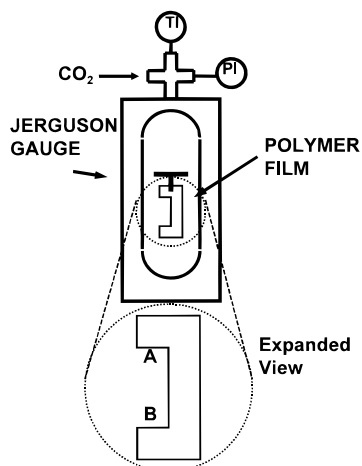


Figure 1. Schematic drawing of the high-pressure swelling apparatus, showing the details of the polymer film.

edges during swelling. The reproducibility of the length measurement was determined to be ± 0.003 cm. A predetermined volume of cosolvent was then injected into the cell, and the length of the polymer film recorded after equilibration. This usually required several hours. The pressure was increased in 4–14-bar increments up to 175 bar; in this manner the concentration of cosolvent was held constant. The length of the polymer film, l , was recorded after several hours to allow for mixing and equilibration. The ratio of swollen polymer volume, V , to original polymer volume, V_0 , was calculated using eq 13.

$$\frac{V}{V_0} = \left(\frac{l}{l_0}\right)^3 \quad (13)$$

This expression assumes that the polymer swells uniformly in all directions. For unoriented rubbery polymers, such as cross-linked PDMS, Fleming and Koros⁵³ verified this assumption. The degree of swelling was also determined while decreasing system pressure in 4–14-bar increments (condition of constant mole fraction of cosolvent).

In Situ Partitioning Experiment. A PDMS film was cut from a clean and dry polymer sheet, as prepared above. The film was cut in the shape of a disk and secured to a window in path I of the dual-path cell; path II contained no polymer film. The temperature was controlled to within ± 0.2 °C using electric cartridge heaters (Omega Technologies Co.) and a model CN9000A temperature controller (Omega Technologies Co.). Prior to any measurements the virgin polymer film was exposed to flowing scCO₂ (41.5 °C and 175 bar) for 15 h to extract any remaining impurities. Blank spectra were measured at 7-bar increments with no cosolvent present through each path. These spectra were used as backgrounds for the spectroscopic determination of the partition coefficient.

The cell was evacuated prior to a partitioning experiment. A predetermined volume of cosolvent was then injected into the cell. The pressure was increased to above the miscibility limit as determined visually in a Jerguson gauge and then increased in 7-bar increments up to 175 bar; in this manner the concentration of cosolvent in the cell was held constant. All FTIR spectra were measured above the miscibility limit of the mixture; therefore condensation on the windows or on the polymer film was prevented. The FTIR spectra via path I (polymer-containing) at each pressure were observed until they were seen to be invariant. This usually required 15–30 min,

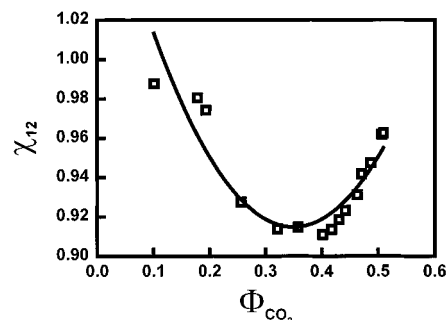


Figure 2. Concentration dependence of interaction parameter for the CO₂–cross-linked PDMS system at 41.5 °C. Concentration units are presented in terms of volume fraction (Φ).

due to the better mixing in the parallel path cell. Spectra were recorded through each path using the backgrounds measured initially. The pressure was then decreased in 4–14-bar increments in order to measure the partition coefficient at constant mole fraction of cosolvent.

Since the partition coefficient is defined as a ratio of cosolvent concentrations between the polymer and fluid phases, eq 10, the polymer film thickness and the distance between the IR windows are required for proper subtraction and determination of the concentration of cosolvent from Beer's law, eq 14.

$$A = \epsilon l C \quad (14)$$

where A is the integrated area of the absorbance band (cm^{-1}), ϵ is the molar absorptivity ($\text{M}^{-1} \text{cm}^{-1}$), l is the path length (cm), and C is the concentration (M). The spectrum of the cosolvent absorbed by the PDMS film was determined by subtracting spectra II (no polymer film) from spectra I (polymer film) using the appropriate subtraction factor. (The background for these spectra were as follows: spectrum I, PDMS film at the desired CO₂ pressure; and spectrum II, desired CO₂ pressure. In this way, any contributions from CO₂ absorbance are minimized.) The subtraction factor was determined from comparison of the blank CO₂ spectra measured previously. Since the concentration of CO₂ at a given density was the same in each path, the ratio of the slopes of the integrated area of a common spectral feature versus CO₂ density yields the subtraction factor. The subtraction factor for all experiments was 0.9585. The length of path II was measured using a Feeler gauge (Starrett Gauge, model 66T). The path length of the unswollen polymer film was determined by measuring the thickness using calipers (Mitutoyo, model 505-637-50). The unswollen thickness was 0.017 ± 0.002 . The change in thickness of the polymer film under experimental conditions was determined from the in situ swelling experiments.

Results and Discussion

Equilibrium Swelling. The equilibrium swelling of the cross-linked PDMS film utilized throughout this work by supercritical carbon dioxide at 41.5 °C is shown in Figure 3 as a function of pressure. The equilibrium swelling is expressed in terms of the ratio of the swollen volume to the original volume. The sigmoidal shape of the swelling curve is consistent with other swelling data available in the literature for cross-linked PDMS.^{47,48} The interaction parameter, χ_{12} , for CO₂/PDMS can be calculated by equating the activity of CO₂ in each phase. The activity of fluid-phase CO₂ as a function of pressure is calculated using the Peng–Robinson equation of state.⁵² The activity of CO₂ absorbed in PDMS is calculated using the Flory–Huggins equation of state, eq 12. A quadratic

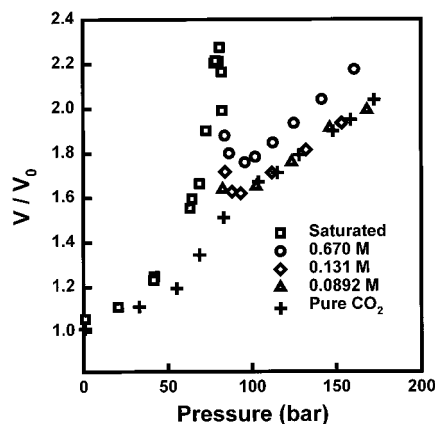


Figure 3. Pressure dependence of the equilibrium swelling of cross-linked PDMS in methanol-modified carbon dioxide. The values listed in the legend are the concentrations of methanol in the fluid phase. The +’s represent the swelling of cross-linked PDMS in pure CO₂.

dependence of the interaction parameter with CO₂ volume fraction (concentration in the polymer) gives the best fit to the swelling data. Concentration-dependent interaction parameters are well-known and should not be surprising.^{45,50,52,54} The result is shown in Figure 2.

The cosolvents utilized in this work are methanol, 2-propanol, and acetone. The swelling behavior of PDMS at 41.5 °C in the presence of carbon dioxide modified with methanol is shown in Figure 3. The square symbols represent swelling under saturated conditions; that is, three phases are present: swollen polymer, liquid, and vapor. The nature of the phase (liquid or vapor) contacting the polymer has no effect on the swelling behavior since the activity of each species in each phase is equal and the equilibrium partitioning should be dependent on the activity. This has been confirmed experimentally. The other symbols represent swelling above the miscibility limit (one phase present) at constant cosolvent concentration or cosolvent mole fraction (as listed in the legend). The most striking feature is the occurrence of a local maximum and minimum in swelling near 80 and 90 bar, respectively. Another interesting feature is that at low cosolvent concentrations, below 0.203 M, very little enhancement in swelling is observed at pressures above 90 bar. Above 0.203 M cosolvent concentration, the degree of swelling is noticeably larger than the pure CO₂ swelling values.

The swelling behaviors of PDMS at 41.5 °C in the presence of carbon dioxide modified with 2-propanol and acetone are shown in Figures 4 and 5, respectively. The square symbols represent swelling under saturated conditions. The other symbols represent swelling above the miscibility limit (one phase present) at constant cosolvent concentration or cosolvent mole fraction (as listed in the legend of each figure). The swelling behaviors are qualitatively similar to that observed in methanol-modified CO₂, i.e. the presence of a local maximum and minimum in swelling. However, the magnitude of the maximum in swelling is 4 and 3 times larger for 2-propanol and acetone, respectively, when compared to methanol. Above 80 bar the swelling behavior is similar for each cosolvent. Surprisingly, the large increase in the maximum in swelling does not lead to large enhancements in swelling at elevated pressures (for the cosolvent concentrations measured).

Spectral Features. Figure 6a,b,c illustrates the procedure for determining the spectrum of cosolvent absorbed in PDMS. This particular example shows the $\nu(\text{O}-\text{D})$ and $\nu(\text{C}-\text{D})$ absorbance peaks of 0.13 M (fluid-phase concentration) methanol (d₄) in scCO₂ at 41.5 °C and 88 bar. Figure 6a,b shows the

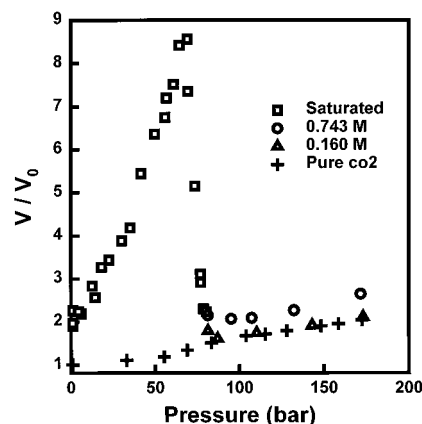


Figure 4. Pressure dependence of the equilibrium swelling of cross-linked PDMS in 2-propanol-modified carbon dioxide. The values listed in the legend are the concentrations of 2-propanol in the fluid phase. The +’s represent the swelling of cross-linked PDMS in pure CO₂.

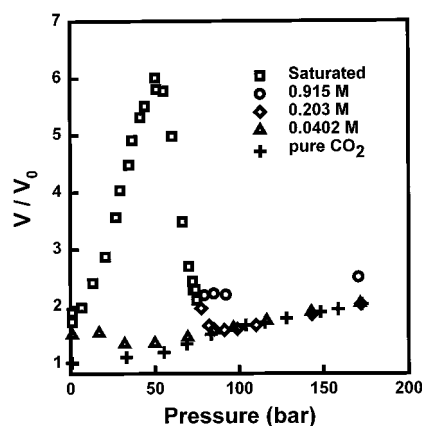


Figure 5. Pressure dependence of the equilibrium swelling of cross-linked PDMS in acetone-modified carbon dioxide. The values listed in the legend are the concentrations of acetone in the fluid phase. The +’s represent the swelling of cross-linked PDMS in pure CO₂.

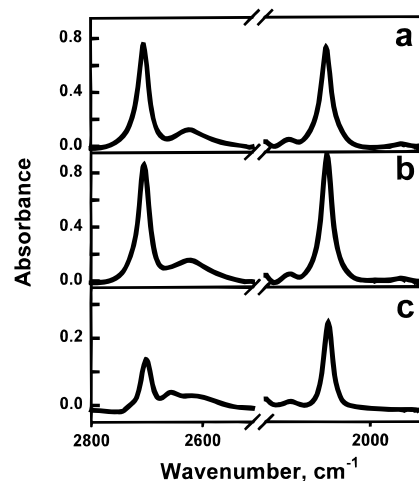


Figure 6. Infrared spectra of the $\nu(\text{O}-\text{D})$ and $\nu(\text{C}-\text{D})$ region of methanol (d₄) at 41.5 °C and 88 bar: (a) fluid-phase spectrum; (b) combined fluid- and polymer-phase spectrum; (c) polymer-phase spectrum resulting from the subtraction of a from b.

spectra measured through paths I and II, respectively. Figure 6c is the spectrum of the absorbed methanol (d₄), which is obtained by subtracting spectrum a from spectrum b. Figure 6a (fluid phase) shows two absorption bands at 2705.2 and 2624.6 cm⁻¹ in the $\nu(\text{O}-\text{D})$ region, which indicates the formation of clusters of self-associated via D-bonding methanol

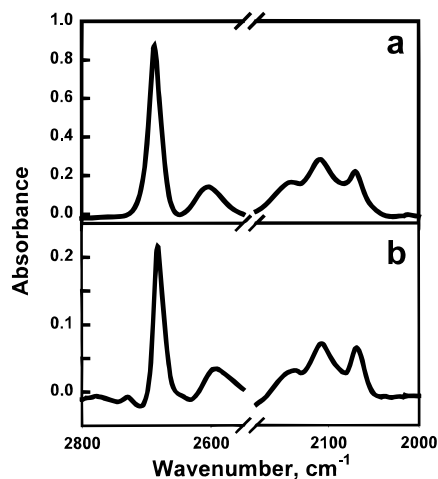


Figure 7. Infrared spectra of the $\nu(\text{O-D})$ and $\nu(\text{C-D})$ region of 2-propanol (d_8) at 41.5 °C and 87 bar: (a) fluid-phase spectrum; (b) polymer-phase spectrum.

(d_4).²¹ However, the polymer-phase spectrum is more complex. Three absorption bands at 2701.3, 2657.9, and 2614.8 cm^{-1} in the $\nu(\text{O-D})$ region are observed. The absorption band at 2657.9 cm^{-1} may represent the formation of a D-bonded methanol (d_4) in with the basic sites in the polymer. Yoshikawa and Matsuura⁵⁵ suggested that methanol might play a role as a hydrogen donor toward oxygen atoms in PDMS. Thus, we believe that the band at 2657.9 cm^{-1} provides spectroscopic evidence for intermolecular interaction between methanol and PDMS film. This result also indicates that methanol is adsorbed by PDMS in different molecular states: self-associates of methanol molecules and methanol molecules H-bonded (D-bonded in the case of methanol (d_4)) to PDMS. Comparison of the fluid-phase and polymer-phase $\nu(\text{C-D})$ spectra reveals a 3- cm^{-1} shift to lower wavenumber. This shift may be due to differences in the dielectric constants of the local environments. The $\nu(\text{O-D})$ absorbance peaks are shifted 4 cm^{-1} to lower wavenumber in going from the fluid phase to the polymer phase. This shift can be attributed to the dielectric constant of the local environment.

Figure 7a,b compares the spectra of 0.16 M (fluid-phase concentration) 2-propanol (d_8) in the fluid phase and polymer phase, respectively, at 41.5 °C and 87 bar in the $\nu(\text{O-D})$ and $\nu(\text{C-D})$ region. These spectra reveal features similar to those observed in methanol (d_4). Clusters of 2-propanol are observed in both the polymer and fluid phases. However, the $\nu(\text{O-D})$ region in the polymer phase shows only two absorption peaks (2682.4 and 2594.6 cm^{-1}), indicating the deuterium bonding in each phase constitutes similar size clusters. Comparison of the fluid-phase and polymer-phase $\nu(\text{C-D})$ spectra reveals a 2- cm^{-1} shift to lower wavenumber. The $\nu(\text{O-D})$ absorbance peaks are shifted 5 cm^{-1} to lower wavenumber in going from the fluid phase to the polymer phase. This shift can be attributed to the dielectric constant of the local environment.

The choice of acetone (d_6) gives a unique spectral feature not present in the acetone. The additional atomic mass, due to deuterium, causes a Fermi resonance peak to appear adjacent to the carbonyl stretch.⁵⁶ The presence of this peak in proximity to the carbonyl stretch allows the observation of changes in the dielectric constant of the medium surrounding the acetone (d_6). The molar absorptivity of the $\nu(\text{C=O})$ band is extremely sensitive to the local environment, whereas the Fermi resonance band is relatively insensitive to the local dielectric environment. The result is two absorbance peaks, side-by-side, that serve as an estimate of the local dielectric constant of the cosolvent.

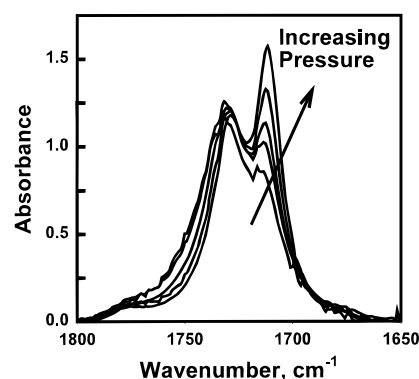


Figure 8. Infrared spectra of the $\nu(\text{C=O})$ region of 0.040 M acetone (d_6) in supercritical CO₂ at 41.5 °C. The arrow shows the behavior of the $\nu(\text{C=O})$ vibration as pressure is increased.

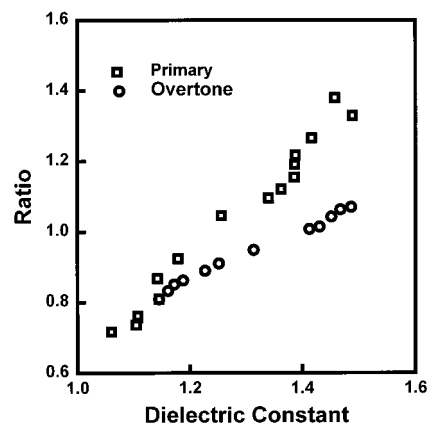


Figure 9. Dependence of the ratio of carbonyl to Fermi absorption bands intensities as a function of CO₂ dielectric constant. The legend shows the absorption bands being utilized.

Therefore, we can estimate the polarity of the fluid phase and stationary phase on the basis of the spectral features of acetone (d_6).

Figure 8 compares the fluid-phase spectra of 0.040 M acetone (d_6) in the $\nu(\text{C=O})$ region at 41.5 °C and increasing system pressure. The intensity of the peak on the right, corresponding to the absorption due to the carbonyl vibration, increases with increasing system pressure, whereas the intensity of the peak on the left, corresponding to a Fermi resonance absorption band,⁵⁶ is relatively unchanged with increasing system pressure. The overtones of these vibration exhibit similar behavior. Forel and Fouassier⁵⁶ show that the ratio of the primary absorption bands is sensitive to the dielectric constant of the solvent. We have plotted the ratio (carbonyl to Fermi) of the intensity for the primary absorption bands and overtones versus dielectric constant of CO₂⁵⁷ in Figure 9. Both sets of data show a linear dependence of the ratio on the dielectric constant. The ratio of overtones is slightly less sensitive to the dielectric constant than the primary absorption ratio. Given these relationships, we can measure the dielectric constant of the local environment from the IR spectrum of acetone (d_6).

Figure 10 compares the spectra of 0.04 M (fluid-phase concentration) acetone (d_6) in the fluid phase and polymer phase at 41.5 °C and 86 bar in the $\nu(\text{C=O})$ region. The most prominent feature is the increase in the intensity of the carbonyl peak relative to the Fermi peak in going from the fluid phase to the polymer phase. Using the correlation from above, the dielectric constant increases from 1.21 in the fluid phase to 1.57 in the polymer phase. This is most probably due to the increased concentration of acetone (d_6) in the polymer phase relative to

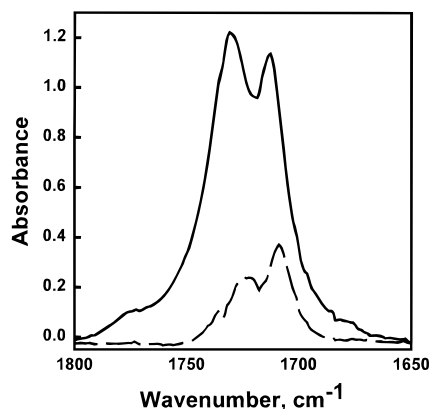


Figure 10. Infrared spectra of the $\nu(\text{C}=\text{O})$ region of acetone (d_6) at 41.5 °C and 86 bar. The solid line represents the spectrum of acetone (d_6) in the fluid phase, and the broken line represents the spectrum of acetone (d_6) absorbed in the polymer phase.

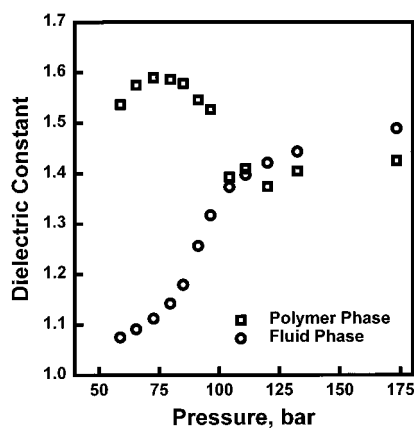


Figure 11. Comparison of the dielectric constant of PDMS and CO_2 as a function of pressure at 41.5 °C, as determined by the ratio of the intensities of the carbonyl and Fermi absorption bands.

the fluid phase. Figure 11 compares the dielectric constant in the polymer phase with the dielectric constant in the fluid phase as a function of pressure in 0.040 M (fluid-phase concentration) acetone (d_6) at 41.5 °C. The fluid-phase dielectric constant increases with pressure. The polymer-phase dielectric constant exhibits a more complex behavior. Below 100 bar the dielectric constant in the polymer phase ranges between 1.5 and 1.6, which is well above the fluid-phase value. Between 100 and 105 bar, the polymer-phase dielectric constant drops to the fluid-phase value and then begins to increase with increasing fluid-phase density. The implications of this are the following: below 105 bar, polar solutes should favor the polymer phase over the fluid phase; and above 105 bar, the polymer and fluid phases are indistinguishable in terms of polarity when acetone is the cosolvent and poly(dimethylsiloxane) is the stationary phase.

Equilibrium Partitioning. All equilibrium partitioning data are presented for pressures above the miscibility limit of the cosolvent and scCO_2 . The equilibrium partitioning data between cross-linked PDMS and scCO_2 at 41.5 °C as a function of pressure with methanol concentration as a parameter are shown in Figure 12. K_c decreases by 1 order of magnitude as the pressure increases from 50 to 175 bar for all concentrations of methanol (d_4) studied. The decrease in K_c is most probably due to the increase in the solvating power of carbon dioxide concomitant with the density increase. Shim and Johnston⁵² observed similar behavior for the partitioning of toluene between scCO_2 and PDMS using inverse supercritical fluid chromatography. The partition coefficient increases as the fluid-phase

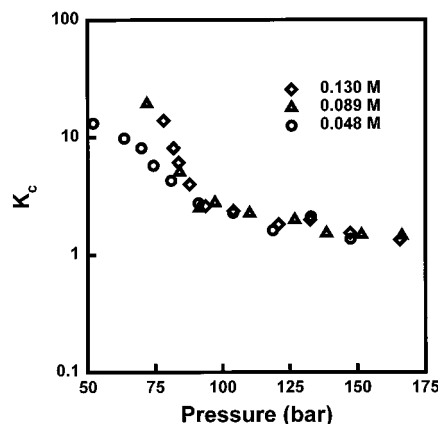


Figure 12. Pressure dependence of the partition coefficient of methanol (d_4) between PDMS and CO_2 at 41.5 °C. The values in the legend are the fluid-phase concentrations.

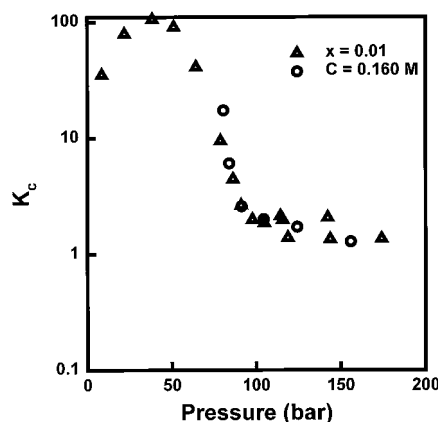


Figure 13. Pressure dependence of the partition coefficient of 2-propanol (d_8) between PDMS and CO_2 at 41.5 °C. The values in the legend state the fluid-phase concentration (circles) and the fluid-phase mole fraction (triangles).

methanol (d_4) concentration increases. However, above 95 bar the partition coefficient is independent of methanol (d_4) concentration.

Figure 13 compares the pressure dependence of the partition coefficient of 2-propanol (d_8) at constant concentration and constant mole fraction. Above 85 bar the partition coefficients are coincident. Below this pressure the partition coefficient becomes composition-dependent. Above 45 bar, K_c decreases as fluid density increases. However, below 45 bar the partition coefficient at constant mole fraction actually increases as fluid density increases, resulting in a maximum. There are two competing effects occurring: at constant mole fraction the molar concentration of alcohol in the fluid phase is actually increasing as the fluid density increases, which would tend to increase the partition coefficient; and increasing density decreases the partition coefficient. Apparently, these two competing effects combine to cause the maximum in K_c .

The pressure dependence of the partition coefficient for acetone (d_6) between carbon dioxide and cross-linked PDMS at 41.5 °C is shown in Figure 14 at two different concentrations and one constant mole fraction. The partition coefficient is independent of fluid composition in the pressure range and compositions studied. K_c decreases monotonically by 2 orders of magnitude in going from the gas region to the supercritical region. The more complex behavior of the alcohols, as compared to acetone (d_6), is most probably due to the ability of the alcohols to self-associate in the fluid and polymer phases.

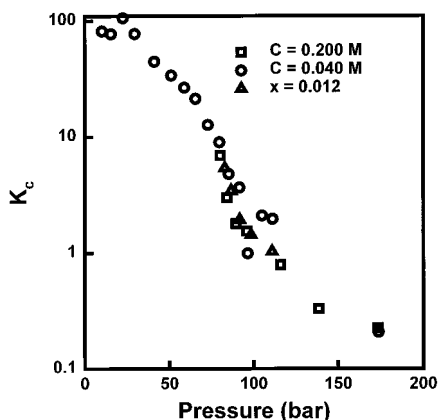


Figure 14. Pressure dependence of the partition coefficient of acetone (d_6) between PDMS and CO₂ at 41.5 °C. The values in the legend state the fluid-phase concentration (circles and squares) and the fluid-phase mole fraction (triangles).

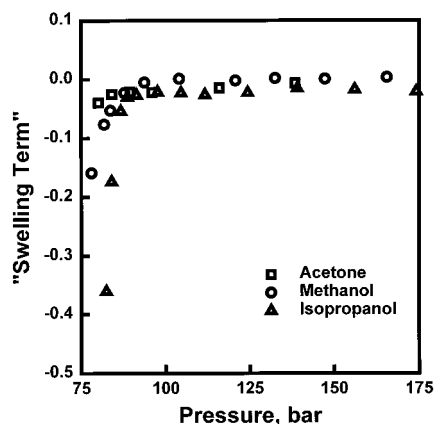


Figure 15. "Swelling term" for PDMS and the three cosolvents at 41.5 °C.

"Swelling Term" and "Chemical Term" Evaluation. The "swelling term", eq 8, for PDMS and the three cosolvents utilized in this work are shown in Figure 15 as a function of pressure at 41.5 °C. The physical conditions used to evaluate the "swelling term" are an open tubular SFC capillary column, 50 μm internal diameter, 1 μm PDMS film thickness, and 3.5 mol % cosolvent. These conditions are similar to those specified by Ekart,⁵⁸ the only difference being the type of stationary phase; Ekart utilized a poly(methyl-*n*-octylsiloxane) stationary phase. Since PDMS and poly(methyl-*n*-octylsiloxane) do not possess any functional groups, their interactions with cosolvents should be similar. Therefore, our comparisons to Ekart's work are qualitative in nature.

Figure 15 shows that above 85 bar the "swelling term" asymptotes near zero for all the cosolvents studied. 2-Propanol has the largest (negative) values that increase in magnitude with decreasing pressure below 85 bar. The "swelling terms" for both methanol and acetone show very little dependence on fluid pressure, except at very low densities. The impact of the "swelling term" is dominated by the ratio of stationary-phase to mobile-phase physical volume. Consequently, the impact of the "swelling term" can be minimized by using large-diameter columns with very thin stationary phases. However, even for the parameters listed here the impact of the "swelling term" is negligible above 85 bar.

The pressure dependence of the derivative of PDMS absorbed cosolvent volume fraction with respect to fluid-phase cosolvent mole fraction ($\partial\phi_{4s}/\partial x_{4m}$) is shown in Figure 16 for the cosolvents studied at 41.5 °C. These profiles reveal a similar

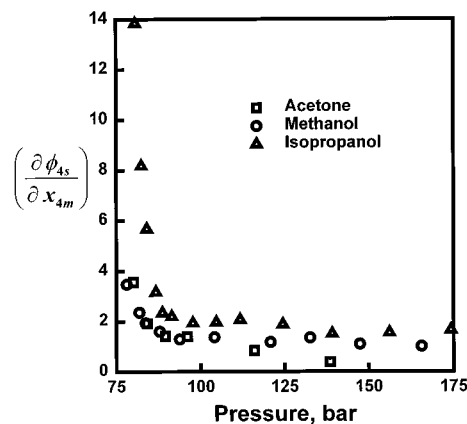


Figure 16. $\partial\phi_{4s}/\partial x_{4m}$ for PDMS and the three cosolvents at 41.5 °C.

trend: decreasing value with increasing pressure and an eventual asymptote above 90 bar. The largest value of the derivative belongs to 2-propanol, with acetone and methanol exhibiting much smaller but similar values in the low-pressure region. The high-pressure asymptotes for each cosolvent are surprisingly similar, with a value of about unity.

Evaluation of the "chemical term", eq 9, requires $\partial\phi_{4s}/\partial x_{4m}$ and the derivative of the chemical potential with respect to the PDMS absorbed cosolvent volume fraction, $\partial\mu_{1s}/\partial\phi_{4s}$. The pressure dependence of the former derivative is presented in Figure 16. The latter derivative is evaluated by differentiating eq 12 with respect to the cosolvent volume fraction for a four-component system. The result is given as eq 15.

$$\left(\frac{\partial\mu_1}{\partial\phi_{4s}}\right) = \frac{\partial \ln \phi_{1s}}{\partial\phi_{4s}} + \frac{\partial(1 - \phi_{1s})}{\partial\phi_{4s}} (\chi_{12}\phi_{2s} + \chi_{13}\phi_{3s} + \chi_{14}\phi_{4s} + 1) + (1 - \phi_{1s}) \left(\chi_{12} \frac{\partial\phi_2}{\partial\phi_{4s}} + \chi_{13} \frac{\partial\phi_3}{\partial\phi_{4s}} + \chi_{14} \right) - \frac{1}{x_4} - \frac{1}{x_2} \frac{\partial\phi_2}{\partial\phi_{4s}} (1 + \chi_{23}\phi_{3s} + \chi_{24}\phi_{4s}) - \frac{\phi_2}{x_2} \left(\chi_{23} \frac{\partial\phi_3}{\partial\phi_{4s}} + \chi_{24} \right) - \frac{1}{x_3} \frac{\partial\phi_3}{\partial\phi_{4s}} (1 + \chi_{34}\phi_{4s}) - \frac{\phi_3}{x_3} \chi_{34} + \frac{\gamma_c \rho_P \bar{V}_1}{2} \left(\frac{1}{3} \phi_2^{-2/3} \frac{\partial\phi_2}{\partial\phi_{4s}} - \frac{1}{2} \frac{\partial\phi_2}{\partial\phi_{4s}} \right) \quad (15)$$

Since the solute is infinitely dilute, ϕ_{1s} is essentially zero and $1 - \phi_{1s}$ retains a value near unity. We also make the assumption that the sorption of CO₂ is not affected by the presence of the cosolvent.⁵³ Equation 16 is the result of including these simplifications.

$$\left(\frac{\partial\mu_1}{\partial\phi_{4s}}\right) = \frac{\partial \ln \phi_{1s}}{\partial\phi_{4s}} + \left(\chi_{12} \frac{\partial\phi_2}{\partial\phi_{4s}} + \chi_{14} \right) - \frac{1}{x_4} - \frac{1}{x_2} \frac{\partial\phi_2}{\partial\phi_{4s}} (1 + \chi_{23}\phi_{3s} + \chi_{24}\phi_{4s}) - \frac{\phi_2}{x_2} \chi_{24} - \frac{\phi_3}{x_3} \chi_{34} + \frac{\gamma_c \rho_P \bar{V}_1}{2} \left(\frac{1}{3} \phi_2^{-2/3} \frac{\partial\phi_2}{\partial\phi_{4s}} - \frac{1}{2} \frac{\partial\phi_2}{\partial\phi_{4s}} \right) \quad (16)$$

Since the "cosolvent effect" for anthracene and 2-naphthol were measured chromatographically by Ekart et al.,⁵⁸ we will evaluate eq 16 for these solutes. The first derivative on the right-hand side of eq 16 cannot be evaluated from our experimental data. However, we can say that it is a positive number, since an increase in cosolvent concentration in the polymer will result in an increase in the solute concentration because of specific interactions between the cosolvent and the solute. The other

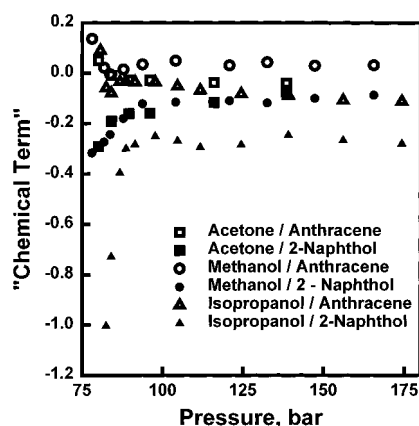


Figure 17. “Chemical term” for PDMS and the three cosolvents at 41.5 °C. The open symbols represent the behavior of anthracene, and the solid symbols represent the behavior of 2-naphthol.

TABLE 1: Summary of Interaction Parameters’ Sources

interaction parameter	source
χ_{12}	assumed to be approximately the same as benzene anthracene: Flory and Shih, 1972 ⁵⁰ 2-naphthol: Flory and Shih, 1972 ⁵⁰
χ_{14}	anthracene: estimated from UNIFAC 2-naphthol: estimated from UNIFAC
χ_{23}	see Figure 2
χ_{24}	determined experimentally from swelling experiments
χ_{34}	determined from isothermal VLE data methanol: Hong and Kobayashi, 1988 ⁶⁶ 2-propanol: Radosz, 1986 ⁶⁷ acetone: Day, Chang, and Chen, 1996 ⁶⁸

volume fraction data are from our current work. Table 1 summarizes the sources for the interaction parameters.

Figure 17 summarizes the “chemical term” for anthracene and 2-naphthol, respectively, as a function of pressure at 41.5 °C with cosolvent as a parameter. (The “chemical term” does not include the increase in volume fraction of the solute due to the increase in cosolvent volume fraction. Therefore these values present the lower bound on the true “chemical term”.) The cosolvent concentration for these figures is 3.5 mol %. The “chemical term” for anthracene is of a smaller magnitude than for 2-naphthol at constant pressure for all cosolvents studied. This is to be expected since anthracene should have weaker specific interactions with the cosolvent; consequently the chemical potential should be less sensitive to the cosolvent concentration in the polymer phase. Above 95 bar the “chemical term” obtains a constant value that depends on the solute and cosolvent combination. Below 90 bar the “chemical term” has a very strong dependence on fluid pressure. This is the region where the cosolvent concentration in the polymer and the swelling of the polymer change the most dramatically. The “chemical term” for 2-naphthol increases with increasing fluid pressure below 90 bar for all cosolvents. The decrease in cosolvent concentration in the polymer may be responsible for this increase. The opposite effect, albeit to a smaller extent, is observed for anthracene. This is most likely due to the changes in the chemical potential due to the swelling of the polymer in this region. The inclusion of $\partial \ln \phi_{1s} / \partial \phi_{4s}$ in the “chemical term” will shift the correction term for 2-naphthol to zero and should have little effect on the anthracene term.

The mixing expansivity term is evaluated using the Peng–Robinson equation of state. The k_{ij} ’s for the equation of state are regressed from P - V - T data⁵⁹ for each cosolvent–CO₂ pair. Using these data along with the quantities determined above,

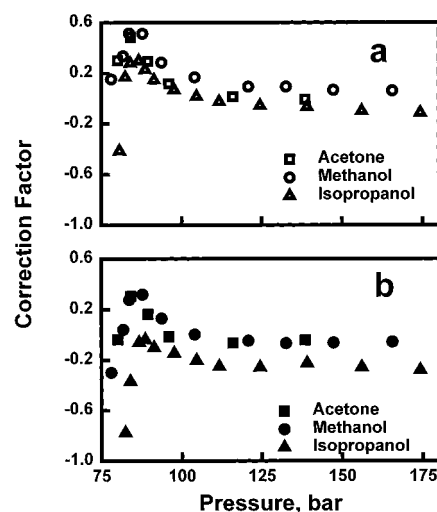


Figure 18. Total correction required to convert retention time data to infinite dilution fugacity coefficients for (a) anthracene and (b) 2-naphthol at 41.5 °C at 3.5 mol % cosolvent concentration.

the total correction to the capacity factor estimate of the cosolvent effect, eq 7, is shown in Figures 18a,b for anthracene and 2-naphthol, respectively, as a function of pressure at 41.5 °C. Both solutes show similar trends for all the cosolvents studied. At low pressure the total correction increases with increasing pressure until a maximum is reached around 85 bar. At higher pressures the total correction decreases and an asymptote is reached above 100 bar. The value of the asymptote depends on the cosolvent–solute pair.

Ekart⁵⁸ reports $\ln(k_1/k_{1,0})$ equals -0.34 for anthracene at 35 °C and 90 bar (15.4 mol/L) and -1.7 for 2-naphthol at 35 °C and 100 bar (16.4 mol/L). Since the solvating power of a supercritical fluid is related to density, we will evaluate the corrections to $\ln(k_1/k_{1,0})$ from Ekart’s work at equivalent densities. The corresponding pressures for anthracene and 2-naphthol at 41.5 °C are 104 and 116 bar, respectively. The corresponding corrections are 0.17 for anthracene and -0.05 for 2-naphthol. This amounts to a 50% correction to the cosolvent effect for anthracene and a negligible -3% correction to the cosolvent effect of 2-naphthol. However, at lower pressure and for other cosolvents the corrections to the capacity factor ratio are much more significant.

The pressure dependence of the capacity factor ratio $k_1/k_{1,0}$ can be estimated by rearranging eq 7. The results for anthracene and 2-naphthol are shown in Figure 19. The ratio of infinite dilution fugacity coefficient data ($\ln(\varphi_{1m}^\infty/\varphi_{1m,0}^\infty)$) in the mobile phase for the open symbols is obtained from Dobbs et al.¹⁴ and Dobbs and Johnston.¹⁵ The filled triangle data are obtained by extrapolating the solubility data.¹⁴ The other values required to calculate the capacity factor ratio are identical to those used to produce Figure 18a,b. The dominating factor in estimating $k_1/k_{1,0}$ at high pressure (above 120 bar) is the ratio of infinite dilution fugacity coefficients (determined from experimental data in this example). However, at lower pressure (80–120 bar) the contribution from the stationary-phase effects becomes more significant. Figure 20 compares the size of the stationary-phase effects correction to the ratio of infinite dilution fugacity coefficients for 2-naphthol in carbon dioxide modified with 3.5 mol % methanol. The stationary-phase effects amount to a 10% adjustment of the ratio of infinite dilution fugacity coefficients above 105 bar. However, at lower pressures (near the critical point) the adjustments are more significant (up to 30% of the measured value) and cannot be neglected.

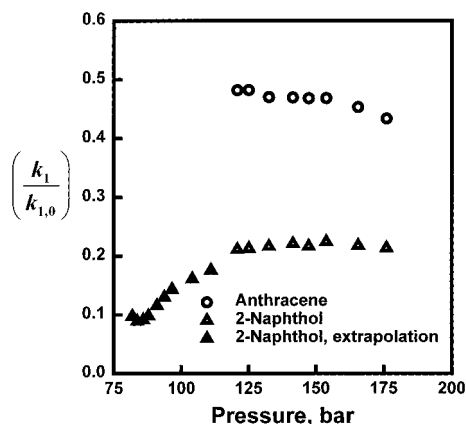


Figure 19. Estimate of cosolvent effect on the capacity factor of anthracene (circles) and 2-naphthol in carbon dioxide modified with 3.5 mol % methanol at 35 °C. The open symbols are estimates using experimental data, and the filled symbols are estimates using extrapolation of experimental data.

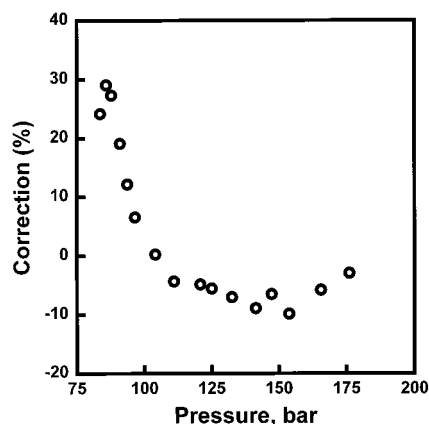


Figure 20. Magnitude of correction to capacity factor ratio with respect to the ratio of infinite dilution fugacity coefficients for 2-naphthol in carbon dioxide modified with 3.5 mol % methanol at 35 °C.

These results indicate that the determination of thermophysical properties via SFC and the estimation of capacity factors require accurate measurement of the swelling behavior of the stationary phase in the presence of cosolvent-modified supercritical fluid, as well as accurate measurement of the partitioning of the cosolvent between the supercritical fluid and the stationary phase. These measurements are both time-consuming and difficult. In addition, the cosolvent effect on the partitioning of the individual solute between the stationary phase and fluid phase is required and may be the most difficult quantity to measure. Clearly, SFC is a powerful analytical tool, and it presents the capability to generate thermophysical data quickly. However, there is no guarantee that these data are accurate, without the determination of the pressure dependence of the swelling and composition of the stationary phase. An equation of state that requires few experimentally determined parameters is required to make accurate determination of thermophysical properties from SFC viable. The desired equation of state should take into account specific interactions, such as hydrogen bonding, between the solute, cosolvent, carbon dioxide, and the polymer. The lattice-fluid models^{60–64} are versatile enough to possibly fulfill these requirements.

Conclusions

The swelling of cross-linked poly(dimethylsiloxane) by cosolvent-modified supercritical carbon dioxide exhibits anomalous

behavior. A relative maximum and minimum in the degree of swelling occur for methanol-, 2-propanol-, and acetone-modified carbon dioxide below 90 bar. Above 90 bar the degree of swelling increases with pressure.

The infrared spectra of methanol (d_4), 2-propanol (d_8), and acetone (d_6) dissolved in the CO₂ fluid phase and absorbed in poly(dimethylsiloxane) are measured in situ. These spectra show evidence for specific interactions between PDMS and the absorbed cosolvent only in the case of methanol. Therefore we believe that dispersion forces are primary responsible for the partitioning of other cosolvents studied between PDMS and CO₂. A special feature of acetone (d_6) is used to measure the local polarity in its environment within PDMS film subjected to cosolvent-modified scCO₂. The local polarity in the polymer phase is higher than in the fluid phase below 100 bar and equal to the polarity of the fluid phase above 100 bar.

The partition coefficients, K_c , of methanol (d_4), 2-propanol (d_8), and acetone (d_6) are reported as a function of pressure in scCO₂ at 41.5 °C. Above 50 bar the partition coefficients of methanol (d_4) and 2-propanol (d_8) decrease with increasing pressure. Below 50 bar the partition coefficient of 2-propanol increases with increasing pressure. The partition coefficient of acetone decreases monotonically with increasing pressure.

The partition coefficient data and swelling data are used, along with the Flory–Huggins equation of state, to estimate the magnitude of the factors influencing the measurement of thermophysical properties from supercritical fluid chromatography. One of the quantities required for the measurement of thermophysical properties from SFC requires the direct measurement of the partitioning of the solute between the polymer phase and the fluid phase. This is beyond the scope of this work. Nevertheless, our results show that the thermophysical properties measured chromatographically required a correction term that depends on the system pressure, the cosolvent, and the specific solute.

The effect of stationary- and mobile-phase phenomena on the capacity factor of 2-naphthol in methanol-modified carbon dioxide is negligible above 105 bar and increases dramatically as the pressure is reduced to near the critical region. These effects are due to the combination of the dramatic swelling of the stationary phase and changes in the chemical potential of the solute in the stationary phase due to partitioning of cosolvent into the stationary phase. The change in compressibility of the mobile phase at constant pressure is also significant and should be included when trying to predict cosolvent effects on capacity factors.

The combined effort of measuring the partition coefficient of cosolvents as a function of pressure, the swelling of the polymer phase as a function of cosolvent and pressure, the partitioning of the solute between the polymer phase and the fluid, and the capacity factor of the solute in SFC might present more work than measuring the solubility of the solute in cosolvent-modified supercritical CO₂. Recently it has been shown that the selectivity in SFC can be affected by partitioning of the cosolvent into stationary phase.⁶⁵ The use of SFC data to measure thermophysical properties of solutes will require an equation of state that can predict the chemical potential of the solute in the stationary phase as well as the partition coefficient of cosolvent and the swelling behavior of the PDMS.

Acknowledgment. We thank E. I. DuPont de Nemours and the U.S. Department of Energy for financial support. We also acknowledge D. M. Bush and greatly appreciate the help of B. Eason, A. R. Stout, and J. Andrews.

Supporting Information Available: The complete set of experimental data presented in the figures are available in tabular form (11 pages). Ordering information is given on any current masthead page.

References and Notes

- (1) Yonker, C. R.; Frye, S. L.; Kalkwarf, D. R.; Smith, R. D. *J. Phys. Chem.* **1986**, *90*, 3022.
- (2) Smith, R. M.; Cocks, S.; Sanagi, M. M.; Briggs, D. A.; Evans, V. G. *Analyst* **1991**, *116*, 1281.
- (3) McHugh, M. A.; Krukoni, V. J. *Supercritical Fluid Extraction—Principles and Practice*; Butterworths-Heinemann: Boston, 1994.
- (4) Ellington, J. B.; Park, K. M.; Brennecke, J. F. *Ind. Eng. Chem. Res.* **1994**, *33*, 965.
- (5) Savage, P. E.; Gopalan, S.; Mizan, T. I.; Martino, C. J.; Brock, E. E. *AIChE J.* **1995**, *41*, 1723.
- (6) Randolph, T. W.; O'Brien, J. A.; Ganapathy, S. *J. Phys. Chem.* **1994**, *98*, 4173.
- (7) Fernandez-Prini, R.; Japas, M. L. *Chem. Soc. Rev.* **1994**, 155.
- (8) Chester, T. L.; Pinkston, J. D.; Raynie, D. E. *Anal. Chem.* **1996**, *68*, 487R.
- (9) DeSimone, J. M.; Maury, E. E.; Menciloglu, Y. Z.; McClain, J. B. *Science* **1994**, *265*, 356.
- (10) Kim, S.; Johnston, K. P. *Ind. Eng. Chem. Res.* **1987**, *26*, 1206.
- (11) Kazarian, S. G.; Gupta, R. B.; Clarke, M. J.; Johnston, K. P.; Poliakov, M. J. *Am. Chem. Soc.* **1993**, *115*, 11099.
- (12) Roberts, C. B.; Zhang, J.; Chateaufneuf, J. E.; Brennecke, J. F. *J. Am. Chem. Soc.* **1993**, *115*, 9576.
- (13) Roberts, C. B.; Zhang, J.; Brennecke, J. F.; Chateaufneuf, J. E. *J. Phys. Chem.* **1993**, *97*, 5618.
- (14) Dobbs, J. M.; Wong, J. M.; Johnston, K. P. *J. Chem. Eng. Data* **1986**, *31*, 303.
- (15) Dobbs, J. M.; Wong, J. M.; Lahiere, R. J.; Johnston, K. P. *Ind. Eng. Chem. Res.* **1987**, *26*, 56.
- (16) Ekart, M. P. Specific Intermolecular Interactions for Tailoring Supercritical Fluid Solutions. Ph.D., University of Illinois at Urbana—Champaign, 1992.
- (17) Levy, J. M.; Ritchey, W. M. *J. High Resolut. Chromatogr. Chromatogr. Commun.* **1985**, *8*, 503.
- (18) Dillow, A. K.; Hafner, K. P.; Yun, J.; Deng, F.; Kazarian, S. G.; Liotta, C. L.; Eckert, C. A. *AIChE J.* **1997**, *43*, 515.
- (19) Lemert, R. M.; Johnston, K. P. *Ind. Eng. Chem. Res.* **1991**, *30*, 1222.
- (20) Strubinger, J. R.; Song, H.; Parcher, J. F. *Anal. Chem.* **1991**, *63*, 104.
- (21) Fulton, J. L.; Yee, G. G.; Smith, R. D. *J. Am. Chem. Soc.* **1991**, *113*, 8327.
- (22) Roth, M. J. *J. Phys. Chem.* **1990**, *94*, 4309.
- (23) Yerrick, K. B.; Beck, H. N. *Rubber Chem. Technol.* **1964**, *37*, 261.
- (24) Yonker, C. R.; Gale, R. W.; Smith, R. D. *J. Phys. Chem.* **1987**, *91*, 3333.
- (25) Bartle, K. D.; Clifford, A. A.; Jafar, S. A. *J. Chem. Eng. Data* **1990**, *35*, 355.
- (26) Brown, B. O.; Kishbaugh, A. J.; Paulaitis, M. E. *Fluid Phase Equilib.* **1987**, *36*, 247.
- (27) Ekart, M. P.; Bennett, K. L.; Eckert, C. A. *ACS Symp. Ser.* **1993**, *514*, 228.
- (28) Gurdial, G. S.; Macnaughton, S. J.; Tomasko, D. L.; Foster, N. R. *Ind. Eng. Chem. Res.* **1993**, *32*, 1488.
- (29) Cygnarowicz, M. L.; Maxwell, R. J.; Seider, W. D. *Fluid Phase Equilib.* **1990**, *59*, 57.
- (30) Van Alsten, J. G. Structural and Functional Effect in Solutions with Pure and Entrainer-Doped Supercritical Solvents. Ph.D., University of Illinois at Urbana—Champaign, 1986.
- (31) Schmitt, W. J.; Reid, R. C. *J. Chem. Eng. Data* **1986**, *31*, 204.
- (32) Eckert, C. A.; Ziger, D. H.; Johnston, K. P.; Kim, S. *J. Phys. Chem.* **1986**, *31*, 1105.
- (33) Yan, C.; Martire, D. E. *J. Phys. Chem.* **1992**, *96*, 3489.
- (34) Lochmuller, C. H.; Mink, L. P. *J. Chromatogr.* **1987**, *409*, 55.
- (35) Shim, J.; Johnston, K. P. *J. Phys. Chem.* **1991**, *95*, 353.
- (36) Kazarian, S. G.; Vincent, M. F.; West, B. L.; Eckert, C. A. *J. Supercrit. Fluids*, in press.
- (37) Kazarian, S. G.; West, B. L.; Vincent, M. F.; Eckert, C. A. *Am. Lab.* **1997**, *29*, 18B.
- (38) West, B. L.; Kazarian, S. G.; Vincent, M. F.; Brantley, N. H.; Eckert, C. A. *J. Appl. Polym. Sci.*, in press.
- (39) Vincent, M. F.; Kazarian, S. G.; Eckert, C. A. *AIChE J.* **1997**, *43*, 1838.
- (40) Vigdergauz, M. S.; Lobachev, A. L.; Lobacheva, I. V.; Platonov, I. A. *Russ. Chem. Rev.* **1992**, *61*, 267.
- (41) Jin, D. W.; Nitta, T. *J. Chem. Eng. Jpn.* **1996**, *29*, 708.
- (42) Kazarian, S. G.; Vincent, M. F.; Eckert, C. A. *Rev. Sci. Instrum.* **1996**, *67*, 1586.
- (43) Roth, M. J. *J. Phys. Chem.* **1996**, *100*, 2372.
- (44) Flory, P. J.; Tataru, Y. *J. Polym. Sci. Polym. Phys. Ed.* **1975**, *13*, 683.
- (45) Flory, P. J. *Principles of Polymer Chemistry*; Cornell University Press: Ithaca, 1953.
- (46) Mark, J. E.; Erman, B. *Rubberlike Elasticity: A Molecular Primer*; John Wiley: New York, 1988.
- (47) Tan, Z.; Jaeger, R.; Vancso, G. J. *Polymer* **1994**, *35*, 3230.
- (48) Kazarian, S. G.; Brantley, N. H.; West, B. L.; Vincent, M. F.; Eckert, C. A. *Appl. Spectrosc.* **1997**, *51*, 491.
- (49) Imanishi, Y.; Adachi, K.; Kotaka, T. *J. Chem. Phys.* **1988**, *89*, 7585.
- (50) Flory, P. J.; Shih, H. *Macromolecules* **1972**, *5*, 761.
- (51) Mark, J. E. *J. Phys. Chem.* **1964**, *68*, 1092.
- (52) Shim, J.-J.; Johnston, K. P. *AIChE J.* **1989**, *35*, 1097.
- (53) Fleming, G. K.; Koros, W. J. *Macromolecules* **1986**, *19*, 2285.
- (54) Bahar, I.; Erbil, H. Y.; Baysal, B. M.; Erman, B. *Macromolecules* **1987**, *20*, 1353.
- (55) Yoshikawa, M.; Matsuura, T. *Polymer J.* **1991**, *23*, 1025.
- (56) Forel, M. T.; Fouassier, M. *Spectrochim. Acta* **1967**, *23A*, 1977.
- (57) Ely, J. F.; Haynes, W. M.; Bain, B. C. *J. Chem. Thermodyn.* **1989**, *21*, 879.
- (58) Ekart, M. P.; Bennett, K. L.; Eckert, C. A. Effects of Specific Interactions in Supercritical Fluid Solutions. In *Supercritical Fluid Engineering Science Fundamentals and Applications*; Kiran, E., Brennecke, J. F., Eds.; American Chemical Society: Washington, DC, 1993; p 228.
- (59) Tilly, K. D.; Foster, N. R.; Macnaughton, S. J.; Tomasko, D. L. *Ind. Eng. Chem. Res.* **1994**, *33*, 681.
- (60) Panayiotou, C. G. *Macromolecules* **1987**, *20*, 861.
- (61) Panayiotou, C.; Vera, J. H. *Polymer J.* **1984**, *16*, 89.
- (62) Condo, R. D.; Sumpter, S. R.; Lee, M. L.; Johnston, K. P. *Ind. Eng. Chem. Res.* **1996**, *35*, 1115.
- (63) High, M. S.; Danner, R. P. *AIChE J.* **1990**, *36*, 1625.
- (64) Sanchez, I. C.; Panayiotou, C. G. Equation of State Thermodynamics of Polymer and Related Solutions. In *Models for Thermodynamic and Phase Equilibria Calculations*; Sandler, S. I., Ed.; Marcel Dekker, Inc.: New York, 1993; pp 187–286.
- (65) Cantrell, G. O.; Stringham, R. W.; Blackwell, J. A.; Weckwerth, J. D.; Carr, P. W. *Anal. Chem.* **1996**, *68*, 3645.
- (66) Hong, J. H.; Kobayashi, R. *Fluid Phase Equilib.* **1988**, *41*, 269.
- (67) Radosz, M. *J. Chem. Eng. Data* **1986**, *31*, 43.
- (68) Day, C.-Y.; Chang, C. J.; Chen, C.-Y. *J. Chem. Eng. Data* **1996**, *41*, 839.